

# Thermally Developable Photographic Materials (TDPM): A Review of the State-of-the-Art in Mechanistic Understanding\*

M. R. V. Sahyun†

Department of Chemistry, University of Wisconsin, Eau Claire, Wisconsin 54702

This article reviews recent studies that have revealed much new information about structure and morphology of the interface formed between silver halide and silver carboxylate phases during fabrication of thermally developable photographic materials (TDPM). This information has proved relevant not only to understanding how latent images may form in TDPM, but has also revealed that morphological features of the interface may govern the course of the development reaction as well.

Journal of Imaging Science and Technology 42: 23–30 (1998)

## Introduction

Thermally developed, photosensitive imaging materials (TDPM) have been known for 150 yr.<sup>1</sup> They have been products of commerce for 30 yr. The early history of their development from laboratory curiosities to media with practical sensitometric, image quality, and environmental features alternative to their conventional silver halide counterparts for application in microforms, medical imaging, non-impact printing, and graphic arts has been documented by Shepard<sup>2</sup> and by Morgan.<sup>3</sup> These landmark papers are basically first-person accounts by two of the key inventors in the field. From a mechanistic point of view, the phenomenology of TDPM has been reviewed by Andreev<sup>4a</sup> and Klosterboer<sup>4b</sup> and, somewhat later, but more superficially, by Zavlin and coworkers<sup>5a</sup> and by Goryaev.<sup>5b</sup>

Recently renewed interest in these imaging media has been sparked by the introduction of new TDPM products, e.g., Imation Corporation's DryView medical imaging system. Concomitantly, the recent literature and conference programs have provided a substantial new body of information on the mechanistic aspects of TDPM. It is the purpose of this article to provide an organized survey of this information and, thereby, update the previously available reviews on the topic.

One key feature that has emerged in the new literature<sup>6–9</sup> is the emphasis on the interface formed between the silver halide and silver carboxylate components of TDPM. Accordingly, photosensitivity in TDPM, which allows image recording, is understood to be a characteristic of the entire interface-forming ensemble, rather than of one particular component, e.g., the silver halide grains alone. In support of this view, it has been noted that the silver halide can be substituted with other photocatalysts, including ZnO<sub>2</sub>, TiO<sub>2</sub>, and silver tetrahydrocaryborate

salts, AgAr<sub>4</sub>B (Refs. 2, 10 and 11 respectively). This critical point seems to have been overlooked in the previous reviews of TDPM function,<sup>3–5,12</sup> although first disclosed by Shepard.<sup>2</sup> Another relevant issue is the general experience of workers in the field that conventional methods of chemical sensitization of silver halide emulsions have either no useful effect or a detrimental effect when applied to the silver halide component of TDPM.<sup>13</sup> Silver halide remains the light-sensitive component of choice, however, to confer photographically useful levels of sensitivity in commercial TDPM products. The formation and characterization of the silver halide–silver carboxylate interface and its impact on the photoimaging characteristics of the TDPM will provide the organizing theme for the review.

## Structure of the Silver Carboxylates

**Crystal Structure.** To interpret the structural characteristics of the silver halide–silver carboxylate interface, it is necessary to have a clear picture of the silver carboxylate structure itself. The unit cell of silver carboxylates derived from straight-chain monocarboxylic acids, CH<sub>3</sub>(CH<sub>2</sub>)<sub>n</sub>CO<sub>2</sub>H, has been known<sup>14</sup> since 1949. The general view of these materials is that they comprise puckered planes of carboxylate–ion–coordinated silver ions separated by the organic residues of the carboxylate species. Only the longer chain members of the series are practically useful in the formation of TDPM. However, until recently the detailed crystal structure of only the short chain members was available<sup>15</sup> due to difficulties in growing suitable crystals of the long chain compounds.

Using Ag K-EXAFS, Tolochko and coworkers<sup>16</sup> established the coordination sphere of silver(I) in silver stearate (*n* = 16). They found that silver stearate forms dimers in which the carboxylate groups from two stearate anions and their associated silver ions form an eight-membered coordination ring. In addition, weak coordinate covalent Ag–O bonding is present between adjacent dimers in the ionic plane. The coordination sphere of silver(I) in silver stearate is thus a highly distorted octahedron. A representative cross section of this structure is shown in Fig. 1. In consequence of the silver–oxygen coordination in silver

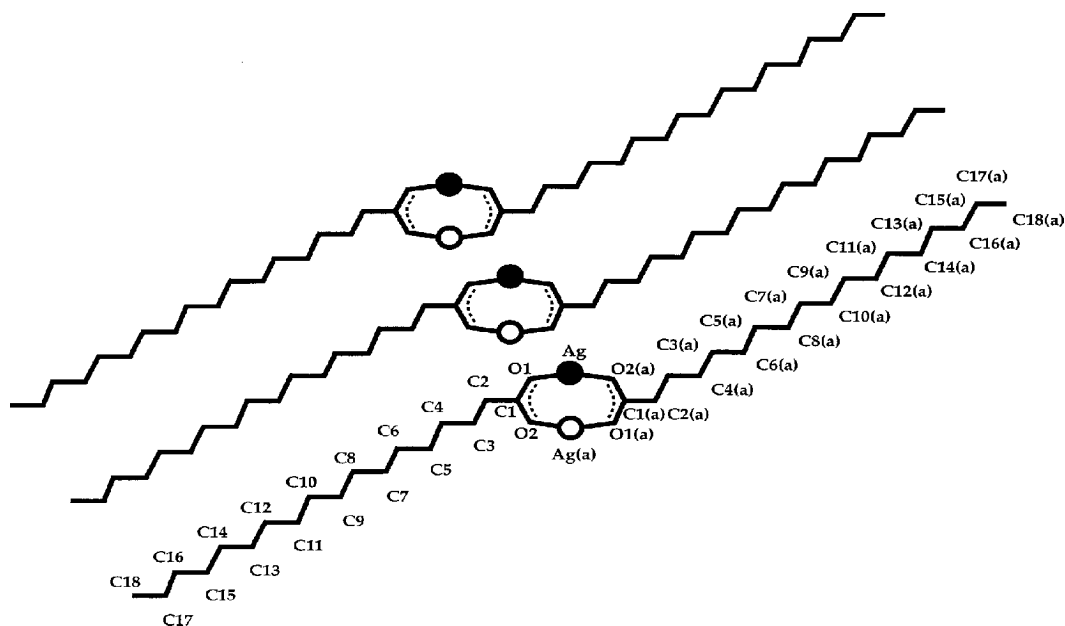
Original manuscript received October 2, 1997

\* Presented in part at the IS&T International Symposium on Silver Halide Imaging, Victoria, B.C., October 27–30, 1997.

† IS&T Fellow

© 1998, IS&T—The Society for Imaging Science and Technology

**Figure 1.** Structure of the silver coordination sphere in silver stearate dimers (Ref. 16a).



stearate, which turned out to be essentially identical to that previously observed by x-ray crystallography for the short chain analogs,<sup>15</sup> the silver stearate dimers are oligomerized to form a two-dimensional coordination polymer, comprising the basal plane (001) of the silver stearate crystal structure. The crystal is accordingly iterated out of a series of such coordination polymer layers, and the interlayer spacing  $d$  has been shown by x-ray diffractometry<sup>17</sup> to be linear with  $n$ .

$$d(\text{\AA}) = 6.55 + 2.38n. \quad (1)$$

**Electronic Structure.** Interesting electronic properties may be associated with this structure. It has been proposed that it will lead to formation of a two-dimensional band structure in the [001] direction, i.e., silver stearate and its homologs should be quasi-two-dimensional ionic semiconductors.<sup>18</sup> This prediction is based on an extended Hückel LCAO MO treatment<sup>19</sup> that predicted *inter alia* a significant degree of Ag–Ag bonding across the eight-membered coordination rings, even before surprisingly short Ag–Ag distances (ca. 2.9 Å, comparable to the interatomic distance in metallic silver) were found in the EXAFS work.<sup>16</sup> The conduction and valence band density of states is accordingly  $10^{19}$  to  $10^{20} \text{ cm}^{-3}$ , depending, of course, on  $n$ . The existence of conduction and valence bands, however, does not necessarily imply significant mobilities for electrons or holes in the silver carboxylates. Dielectric spectroscopy and conductivity measurements<sup>8</sup> suggest, rather, that the long chain silver carboxylates may best be thought of as insulators, typical of ionic solids.

A consequence of the short Ag–Ag bond distances within individual silver carboxylate dimers in this model<sup>18</sup> is that the states at the bottom of the conduction band are localized and can be represented as  $(\text{Ag}_2)^{2+}$ . Formation of development centers, i.e., latent images, in unhalidized silver carboxylates on UV irradiation has been reported.<sup>8</sup> It has also been claimed<sup>20</sup> that certain dyes can extend this sensitivity into the visible regime. Trapping of an electron in one of these conduction band states leads to formation of  $\text{Ag}_2^+$ , a species which has repeatedly been identified as a key intermediate in the nucleation of metallic silver phase formation from a variety of silver-ion-containing systems.<sup>21</sup>

In modern parlance, the coordination polymer plane can be said to form a Peirls-distorted quantum film, and the crystal structure as a whole comprising an array of such quantum films separated by organic dielectric spacers results in a multi-quantum well device.<sup>22</sup> The silver carboxylates of imaging utility are all long chain ( $n \geq 12$ ) complexes for which  $d \geq 35 \text{ \AA}$ . Under these conditions little or no exciton exchange would be expected between the band-forming layers, nor should there be significant carrier mobility in a direction normal to the (001) plane.<sup>23</sup>

A test of the electronic structure hypothesized to correspond to the crystal structure comes from the absorption edge analysis of silver carboxylates. The absorption spectrum for silver stearate ( $n = 16$ ), obtained by diffuse reflection spectroscopy followed by a Kubelka-Munk transform<sup>24</sup> is shown in Fig. 2(a). Its analysis as a plot [Fig. 2(b)] of the square root of the absorption coefficient  $k^{0.5}$  as a function of photon energy  $h\nu$  is linear, characteristic of an indirect band semiconductor,<sup>25</sup> with an optical band gap of  $3.83 \pm 0.025 \text{ eV}$ .

It has also been shown<sup>8</sup> that silver stearate can be synthesized by reaction of silver halide with sodium stearate. When we treated a silver iodobromide nanosol<sup>26</sup> with sodium stearate (both  $10^{-4} \text{ M}$  in ethanol), we could follow the reaction by luminescence spectroscopy at room temperature.<sup>27a</sup> Excitation and emission spectra are shown in Fig. 3. The energy of the excitation maximum is 3.78 eV, in good agreement with the band gap for silver stearate inferred from absorption spectroscopy. Emission is centered at 3.35 eV, which may correspond to a localized state in the region of lattice distortion, i.e., the interfacial zone (see below), or an iodide cluster in the silver halide phase.<sup>26,27b</sup> Similar inhomogeneous broadening of both excitation and emission bands (ca.  $3200 \text{ cm}^{-1}$ ) suggests that the former interpretation is the more plausible. This photoemission was not observed in either the nanosol, by itself, nor in independently synthesized silver stearate.

### Formation of the Photosensitive Interface

In the production of TDPM the juxtaposition of silver halide and silver carboxylate phases may be achieved in one of two ways<sup>4,7,8,28</sup>:

- (1) preformed systems, in which silver carboxylate is synthesized in the presence of silver halide microcrystals;

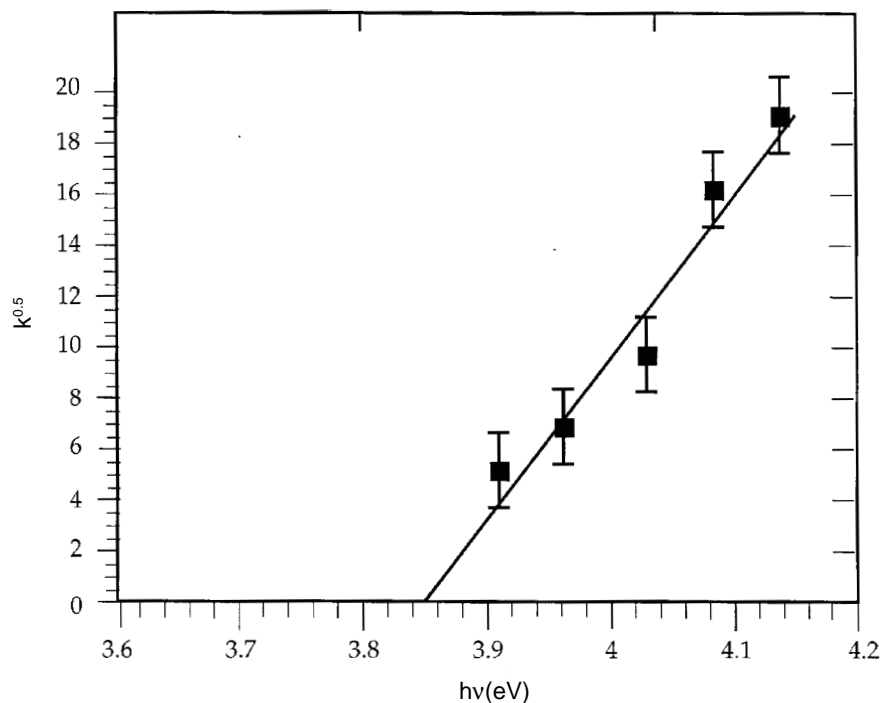
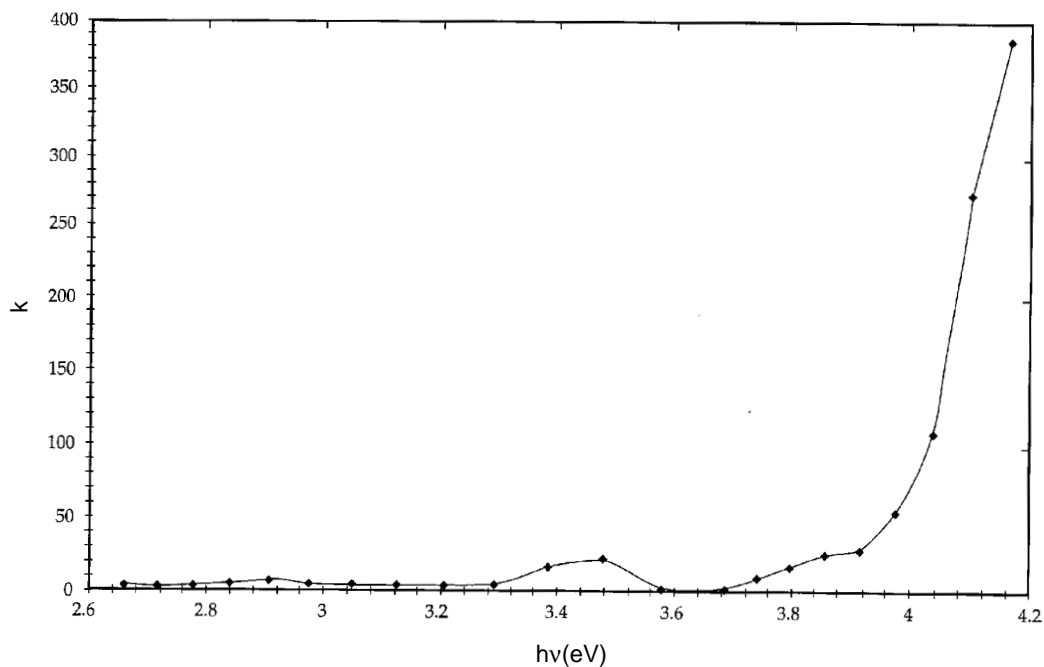


**Figure 2.** (a) Absorption spectrum of silver stearate and (b) determination of silver stearate optical band gap from spectroscopic data (Ref. 24).

- (2) in situ systems, in which silver carboxylate is converted, in part, to silver halide by use of an appropriate halidizing agent.

Using TEM and SEM, Bokhonov and coworkers<sup>7</sup> have studied morphological regularities in the formation of silver halides during in situ halidization of silver stearate. It was found with most halidizing reagents of usual practice, e.g.,  $\text{CaBr}_2$ ,  $\text{KBr}$ ,  $\text{KI}$ , etc., that conversion occurred on the lateral faces of the silver stearate crystals, corresponding to, e.g., the (010) crystal plane, which are intersected by the ionic coordination polymer (001) planes. Ionic mo-

bility in these latter planes provides a mechanism for delivering silver ions to the reactive sites during the process of interface synthesis. This result implies substantial interstitial silver ion mobility in the silver carboxylate phase at room temperature and above, as already inferred by Khainovskii and coworkers<sup>8b</sup> on the basis of conductivity studies.

High-resolution TEM imaging provided graphic evidence for possible epitaxial character of the silver halide–silver carboxylate interface.<sup>7</sup> Under specially controlled conditions of in situ halidization employing  $\text{CaBr}_2$  as the halidizing reagent, the silver halide crystals grew so that

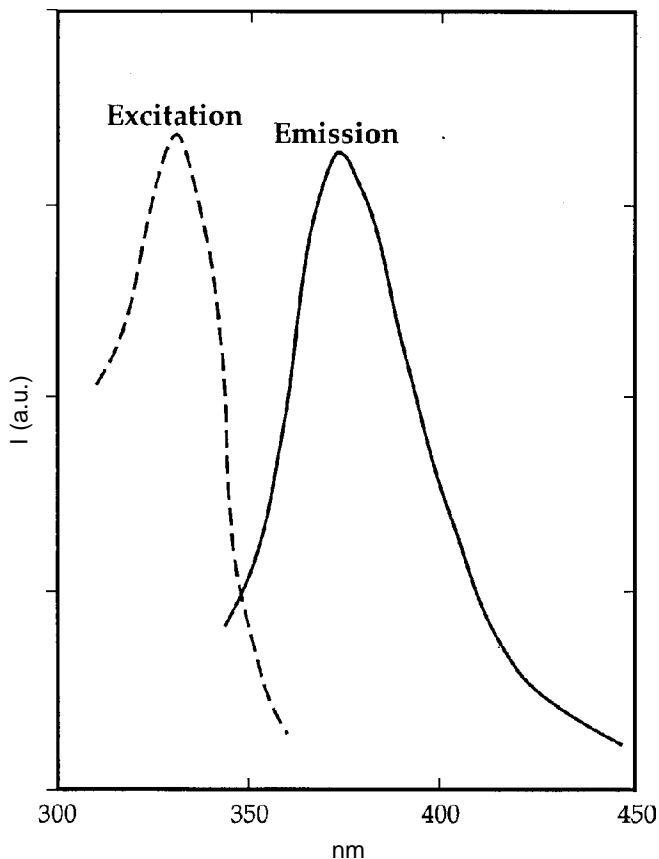


**Figure 3.** Excitation and photoluminescence spectra assigned to (see text) the silver stearate–silver bromide preformed interface.

silver halide (100) planes became extensions of the silver stearate (001) plane. In the zone of contact between the crystals, distortion to accommodate the lattice mismatch between the phases was seen to occur in the silver stearate phase. These features are shown in Fig. 4.

Metathetical synthesis of silver stearate and its in situ halidization have been monitored potentiometrically.<sup>29</sup> The

redox potential (versus SCE) of an aqueous silver stearate dispersion was found to approach an equilibrium value of +0.45 V, which is decreased to a stable value of ca. +0.21 V when the available reactive sites on the silver stearate are saturated with bromide (ca. 50% conversion). The former value corresponds to a  $pAg = ca. 1.5$  and presumably defines the Fermi level of the unhalidized silver carboxylate phase. The equilibrium silver ion potential for halidized silver stearate corresponds to  $pAg = 5.5$ .

The process of preformed interface synthesis can be simulated by reaction of AgBr with sodium stearate. Using high-resolution TEM, Bokhonov and coworkers<sup>8</sup> found that this procedure led to a different sort of epitaxy in which (001) silver stearate planes formed on, and parallel with, silver bromide (111) faces. This situation is shown in Fig. 5. Significant distortions of the interlayer spacing from the value expected for silver stearate<sup>17</sup> are not apparent in the fringes observable within the interfacial zone in this image, but may occur within its (001) plane. This structure should correspond to the experimental situation for which the photoemission spectra were obtained (Fig. 3).

### Photophysics of the Silver Halide–Silver Carboxylate Interface

**Heterojunction Formation.** The epitaxial structures shown in Figs. 4 and 5 should give rise to a heterojunction, as shown schematically in Figs. 6(a) and 6(b). This diagram implies the following assumptions:

- (1) both solids are insulators at room temperature;
- (2) accordingly, the Fermi levels are located in the middle of the band gaps in both cases;
- (3) all-band bending occurs on the silver carboxylate side of the interface.

This last assumption can be justified on the grounds that the silver halide grains used in practical TDPM are usually very small in size (0.01 to 0.1  $\mu m$ ),<sup>4,29</sup> hence unlikely to support significant band bending. The ca. 0.4-eV mismatch between the Fermi levels of silver carboxylate (*vide infra*) and silver bromide<sup>30</sup> [Fig. 6(a)] thus results in a downward bending of the silver carboxylate bands at the interface.

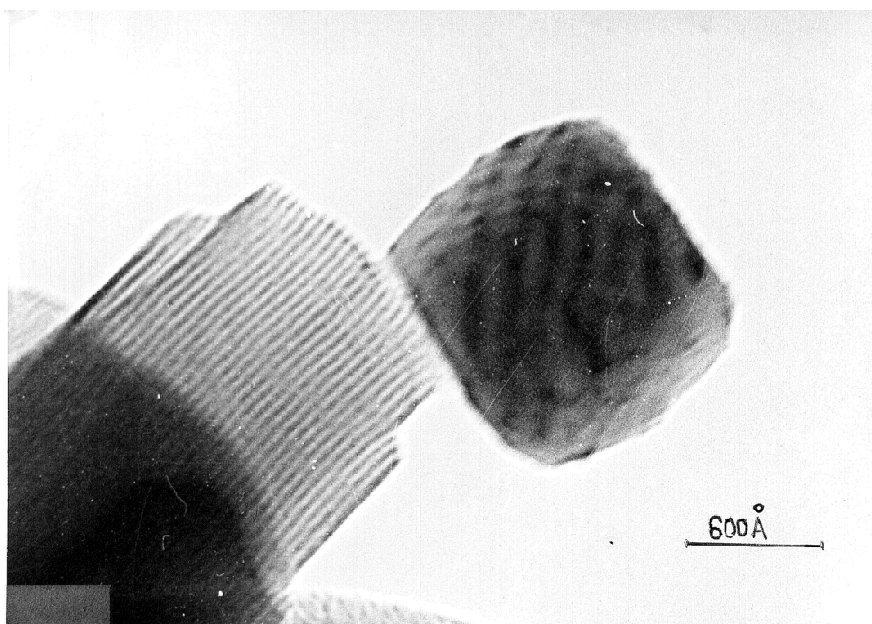


**Figure 4.** High-resolution TEM image of the interface produced by in situ halidization of silver stearate with  $CaBr_2$  (Ref. 7).

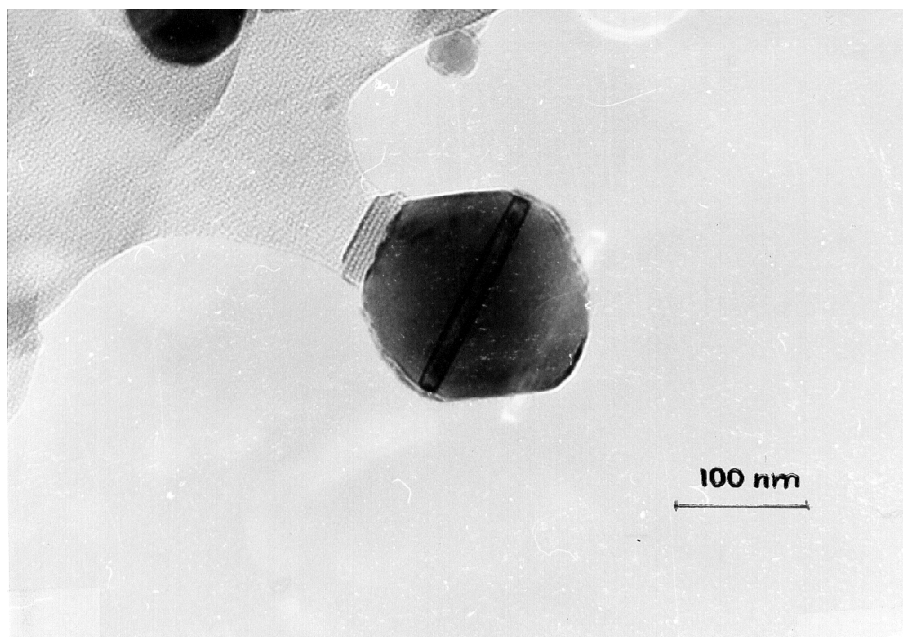


**Figure 5.** High-resolution TEM of preformed silver bromide-silver stearate interface (Ref. 8).

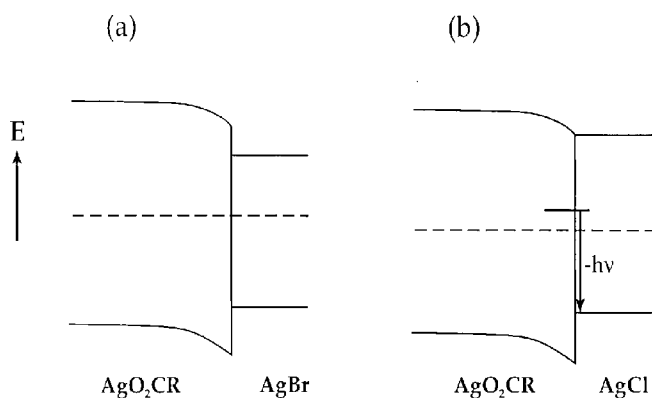


**Figure 6.** Schematic energy level diagrams of the heterojunctions corresponding to the silver carboxylate-silver halide interface: (a) silver bromide, (b) silver chloride.

Given low densities of states in the silver carboxylate phase<sup>18</sup> and the accordingly low mobilities for electronic carriers therein, it is reasonable to associate this band bending with accumulation of mobile silver ions at the interface. This hypothesized, localized nonstoichiometry gives rise to a unique signature for the interface in the dielectric absorption spectrum of the silver halide-silver carboxylate system.<sup>8</sup> The uncompensated silver ion states allow electron trapping to occur across the interface. The interface thus effectively separates electron-hole pairs photogenerated in the silver halide phase, because no energetically viable pathway exists for photoholes to transport into the silver carboxylate phase.

This interface phenomenology is the basis for the “photocatalytic” mechanism of latent image formation in TDPM introduced by Zou and coworkers.<sup>6</sup> This mechanism was invoked to rationalize the silver halide grain size independence of photocharge signals for silver halide-silver carboxylate systems as well as the inapplicability of conventional silver halide chemical sensitization schemes to the enhancement of photosensitivity of TDPM. These doping strategies are designed *grosso modo* to introduce deep electron or hole traps that thereby facilitate electron-hole

separation within the silver halide phase,<sup>30</sup> but are superfluous in the presence of the heterojunctions as illustrated in Fig. 6.

Figure 6(b) illustrates the analogous silver chloride-silver carboxylate heterojunction. Formation of this heterojunction is accompanied by observation of a new band centered on 590 nm in the low-temperature photoluminescence emission spectrum.<sup>8</sup> As shown in the diagram, this emission can be assigned to free hole-trapped electron recombination at the interface. The distribution of deep electron trapping states is accordingly centered ca. 0.4 eV above the silver carboxylate Fermi level. A corresponding red (ca. 675 nm) emission might be expected from the silver bromide-silver carboxylate system, but has not yet been reported. These emission bands may, however, not be observed at room temperature, insofar as the deep trapped electrons may be consumed in latent image formation. Alternatively, free hole-trapped electron recombination may then occur as an activated, radiationless multiphonon transition.<sup>31</sup>

**Latent Image Formation.** In the previous literature on TDPM it has been tacitly assumed that the photochemically generated, developable latent image comprises some sort of silver cluster, by analogy to conventional silver halide photography.<sup>1-6,12,13</sup> Yet the experimental evidence in support of this hypothesis has been minimal. On the contrary, it was shown by Morgan (cited in Ref. 2) that synthesis of a preformed TDPM using a fogged silver halide emulsion did not affect sensitometry or developability of the TDPM vis-a-vis a material synthesized with a scrupulously fog free silver halide component.

Recently we reported<sup>6</sup> results of laser flash photolysis of a silver bromide nanoparticle dispersion,<sup>26</sup> synthesized without and with a silver stearate interface. The transient absorption spectra recorded 0.2 to 5 ns after photolysis at 355 nm are shown in Figs. 7(a) and 7(b). In both cases the transient absorptions can be assigned to formation of silver(0) clusters, for which the silver plasmon resonance absorption<sup>32</sup> at 400 to 450 nm is diagnostic. However, significant differences exist in both the kinetics of appearance of the transients and their spectral distribution in the two cases. From this experiment we can infer that,

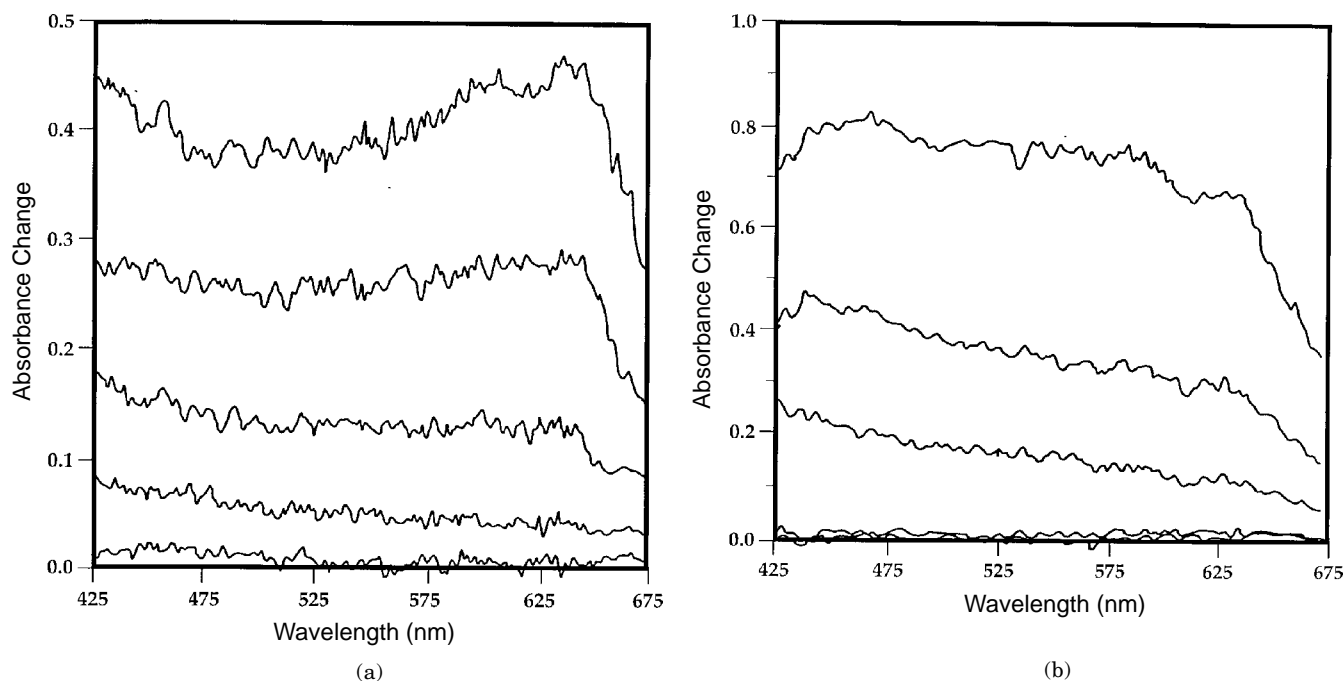


**Figure 7.** Transient absorption spectra at various delay times following laser flash photolysis (355-nm, 30-ps FWHM) of silver bromide nanosol: (a) as synthesized; spectra (bottom to top) correspond to 0.05-, 0.2-, 0.5-, 1-, and 2-ns delays; (b) with silver stearate interface formed by treatment of the starting nanosol with sodium stearate; spectra (bottom to top) correspond to 0.2-, 0.5-, 1-, 2-, and 5-ns delays (Ref. 6).

like silver bromide itself, the silver bromide–silver carboxylate interface is photochemically reactive, leading to separation of a silver(0) phase but that the morphology of the photoproduct is somewhat different in the two cases.

The transients observed for the unmodified silver bromide nanoparticles [Fig. 7(a)] strongly resemble those reported<sup>33</sup> for conventional silver bromide and iodobromide emulsions under similar conditions. Broad spectral absorption of silver formed by photolysis of silver halides has been reported in the case of photochromic glasses.<sup>34</sup> In both these media a second long-wavelength contribution to the absorption spectrum has been observed and assigned to a transition of the silver–silver halide interface,<sup>35</sup> i.e., from the silver(0)-filled continuum of states to the silver halide conduction band at the interface. This is the same transition assigned to the Herschel effect in conventional photography<sup>36</sup> and presumably responsible for the dependence of the color of photolytic silver on the halide composition of the silver halide from which it is generated.<sup>37</sup> This transition is substantially quenched when photolysis occurs with the silver bromide interfaced with silver stearate, as shown in Fig. 7(b). This result implies that the silver(0) photoproduct, and, by extrapolation, the latent image in TDPM, is not largely formed in intimate juxtaposition with the silver halide phase. This inference is consistent with the photocatalytic model of interface photolysis,<sup>6</sup> but not with the frequently cited<sup>1–5</sup> assumption that the silver halide component itself forms the latent image in TDPM.

### Thermal Development Mechanisms in TDPM

**Background.** Early TDPM relied on thermolysis of the silver carboxylate component for amplification of the photocatalytically generated latent image.<sup>4,17,38</sup> Modern materials include developing agents, usually hindered phenols,<sup>2,4</sup> and silver ion complexing agents, e.g., phthalazine, phthalimide, etc., that promote the reaction.<sup>4,16a,29</sup> One of the controversial questions with regard to the mechanistic function of TDPM has been whether,

under these conditions, silver ions from the silver halide component as well as from the silver carboxylate become reduced. Zavlin<sup>5a</sup> specifically states that the reducing agent develops the silver halide component, while Klosterboer<sup>4</sup> denies this proposition, largely on the basis of Morgan's reported observations.<sup>3</sup> This discrepancy may be accounted for in part by the wide variety of TDPM formulations used both commercially and in experimental investigations over the past 30 yr. It seems now generally agreed<sup>18,29,39</sup> that in modern commercial TDPM the silver carboxylate is the only source of silver ions for the image-forming redox reaction.

Up until now, physical development in conventional photography has provided the only paradigm for description of the development process in TDPM.<sup>4</sup> Accordingly the reaction is thought to proceed in a two-step fashion:<sup>16a,39</sup>

- (1) conversion of the silver carboxylate to a silver complex that has high mobility in the reaction medium
- (2) diffusion of the silver complex to the development center where it is reduced to metallic silver.

It has been proposed that molten fatty acid, which is a by-product of step 1 at the development temperature, may be the reaction medium.<sup>40</sup> Activation parameters determined in kinetic studies also suggest that in the second step decomposition of the complex and one-electron reduction of silver ion occur in concerted fashion.<sup>39</sup>

**Kinetic Studies.** The kinetic studies<sup>39,41</sup> have also shown that the basis for more rapid initiation of development in exposed areas of a TDPM is a more positive entropy of activation for the development reaction compared to unexposed areas. By comparison, in conventional photographic development, image–fog discrimination is usually thought to be based on a differential in enthalpy of activation.<sup>42</sup> One possible physical interpretation of this result is simply the presence of more nucleation sites for the metallic silver phase forming reaction, i.e., development centers, where the TDPM has been light exposed.

At the same time attempts at computer simulation of development kinetics based on this interpretation and assuming the two-step model above have had, at best, limited success.<sup>39</sup> One reason is now apparent: namely, this oversimplified picture has failed to take into account the operation of other reactions, e.g., further complex forming reactions. Such chemistry tends to make silver ions less available for reduction to silver and operates in competition with the reduction reaction.<sup>43</sup> This situation tends to reduce contrast in the TDPM and improve image-background discrimination, but also may reduce the efficiency of silver utilization in image formation. It furthermore may contribute to shelf instability of the TDPM and/or lead to artifactual results in Arrhenius testing of TDPM, insofar as the reactions operate, albeit slowly, at temperatures well below development temperature.<sup>43</sup>

Arrested development of TDPM probed by TEM<sup>39</sup> has shown that nucleation of development, i.e., formation of new development centers, continues to occur over the course of the reaction. Thus, many more development centers than silver halide grains may be present in an exposed region of the TDPM. These centers are not necessarily juxtaposed to the silver halide grains. Thus, secondary nucleation of the phase-forming reaction continues to increase the multiplicity of reaction sites, thereby further reducing the entropy of activation of the reaction. As a consequence, positive feedback,<sup>44</sup> i.e., pseudo-autocatalytic kinetics,<sup>41</sup> is observed in the development reaction. The mechanism of formation of the secondary development centers is not clear from the published reports, however. It has been demonstrated with certain developing agents<sup>41,45</sup> that infectious development may be obtained in TDPM. We accordingly speculate that an infectious component to development may exist with the conventionally used hindered phenolic developers, just as an infectious component to direct chemical development often exists in conventional silver halide photography, e.g., when normal MQ developers are employed.<sup>46</sup>

A further consequence of this mechanism of development is that higher levels of density, whether the result of longer development time or higher exposure, correspond to formation within a given volume of the TDPM of more particles of metallic silver, rather than just larger ones.<sup>39</sup> In this regard, silver ion reduction in the TDPM is much like the process occurring in other colloidal silver forming systems, e.g., the reduction of aqueous silver ion by *p*-phenylenediamine and by Eriochrome T and the base-catalyzed formation of colloidal silver in silver ion containing isopropanol solution (Refs. 47, 48, and 49, respectively). Because the number of reduced silver particles rather than their size increases with development time, development of TDPM corresponds to the so-called "granular" limiting case of conventional photographic development,<sup>50</sup> with expected consequences on image quality and detective quantum efficiency of the TDPM.<sup>51</sup>

More massive deposits of image-forming silver can result by aggregation of these "elementary," spheroidal particles to form complex, fractal deposits.<sup>39</sup> These aggregates correspond to a black appearance of the reduced silver (neutral image tone), compared to the yellow-brown color characteristic of the silver plasmon resonance absorption of spheroidal, colloidal silver deposits.<sup>32</sup> Adsorption of the silver complexing reagents to the spheroidal particles formed in the primary development reaction may mediate their aggregation, thus accounting for the apparent function of these compounds as "toners".<sup>4</sup>

**Influence of the Interface.** Recently, Bokhonov and coworkers<sup>9</sup> have shown that the morphology of the silver de-

posit formed on development of a TDPM may reflect the mode of formation of the photosensitive silver halide-silver carboxylate interface. Thus, when the interface is preformed, typical deposits formed by aggregation of spheroidal particles are consistently observed. In the case of in situ halidization filamentary silver may result. (Depending on the particular TDPM formulation employed, however, this is not always the case<sup>29,39</sup>). In silver halide photography, filamentary silver formation is usually associated with "direct development" and spheroidal silver deposits are usually associated with "physical development." In real systems, both mechanisms may operate in parallel.<sup>52</sup>

The classical mechanism of filamentary silver formation in conventional photographic development<sup>53</sup> posits rate-limiting diffusion of silver ions in the silver halide crystal to a small region of the interface with the development center where reduction occurs. Recall that under conditions of in situ halidization, the silver halide grains form on the lateral planes of the silver carboxylate crystal (see Fig. 4). The formation of silver halide nanocrystals at these sites implied transport of silver ion to the reactive site along the (001) ionic planes of the silver carboxylate, i.e., significant silver ion mobility along these planes (see above). Photocatalytically generated latent image centers in these systems should be similarly situated: the mechanism of latent image formation reviewed above implies that these centers will form in the interfacial zone that may extend only a few tens of angstroms from the silver halide phase itself.<sup>7</sup> As in the case of conventional silver halide photography under conditions of silver ion transport limitation, electrons transferred to the growing metallic silver center from the developing agent can reduce mobile silver ions transported to the reaction site along the ionic layer of the silver carboxylate phase with similar morphological consequences. This proposal<sup>54</sup> corresponds to a "direct development" mechanism for silver carboxylate. Under given conditions of silver halide-silver carboxylate interface morphology and, presumably, complexing agent concentration, it may operate in parallel with the well-established "physical development" pathway.<sup>4,39</sup> The mechanism of development in TDPM accordingly reflects the morphology of the original silver halide-silver carboxylate interface.

## Conclusions

Recent studies have revealed much new information about structure and morphology of the interface formed between silver halide and silver carboxylate phases formed in the fabrication of TDPM. This information has proved relevant not only to understanding how latent images may form in TDPM, but has also revealed that morphological features of this interface may govern the course of the development reaction as well. ▲

**Acknowledgment.** The author wishes to thank Drs. D. R. Whitcomb, Imation Corp., and L. P. Burleva, Institute for Solid State Chemistry, Russian Academy of Sciences, for helpful discussion, and especially for assistance with and analysis of the Russian literature. The work of preparing this review was supported by a grant from the Imation Corp. Figures 1, 4, 5, and 7 are reproduced with kind permission of the copyright holder, the Society for Imaging Science and Technology (IS&T).

## References

1. W. H. Fox Talbot, U.S. Patent 5,171 (1847).
2. J. W. Shepard, *J. Appl. Photogr. Eng.* **8**, 210 (1982).
3. D. A. Morgan, *J. Imaging Technol.* **13**, 4 (1987); *Proc. SPIE* **1253**, 239 (1990).

4. (a) V. M. Andreev, E. P. Fokin, Yu. I. Mikhailov, and V. V. Boldyrev, *Zhur. Nauch. i Prikl. Fotogr. i Kinematogr.* **24**, 311 (1979); (b) D. H. Klosterboer, in *Imaging Materials and Processes*, 8th ed., J. M. Sturge, V. Walworth, and A. Shepp, Eds., Van Nostrand-Reinhold, New York, 1989, Chap. 9.
5. (a) P. M. Zavlin, A. N. Dyakonov, S. S. Mnatsakanov, S. S. Tibilov, P. Z. Velinzon, and S. T. Gaft, *Tekh. Kino. Telev. Nauka i Tekhnika* **9** (1990); see also *Proceedings: IS&T's 49th Annual Conference* (IS&T, Springfield, VA, 1996), pp. 422ff.; (b) M. A. Goryaev, *Zhur. Nauch. i Prikl. Fotogr. i Kinematogr.* **36**, 421 (1991).
6. C. Zou, M. R. V. Sahyun, B. Levy, and N. Serpone, *J. Imaging Sci. Tech.* **40**, 94 (1996).
7. B. B. Bokhonov, L. P. Burleva, W. C. Frank, J. R. Miller, M. B. Mizen, M. R. V. Sahyun, D. R. Whitcomb, J. M. Winslow, and C. Zou, *J. Imaging Sci. Tech.* **40**, 85 (1996).
8. (a) B. B. Bokhonov, L. P. Burleva, A. A. Politov, N. F. Uvaraov, D. R. Whitcomb, M. B. Mizen, and M. R. V. Sahyun, *Proceedings: IS&T's 50th Annual Conference*, IS&T, Springfield, VA, 1997, pp. 38ff.; (b) N. G. Khainovskii, E. F. Khairetdinov and V. M. Andreev, *Izv. Sib. Otd. Nauk, SSSR, Ser. Khim. Nauk.*, **5**, 34 (1985).
9. B. B. Bokhonov, L. P. Burleva, W. C. Frank, M. B. Mizen, D. R. Whitcomb, J. Winslow, and C. Zou, *J. Imaging Sci. Tech.* **40**, 417 (1996).
10. J. J. A. Robillard, Fr. Patent 2,254,047 (1973).
11. M. R. V. Sahyun, R. C. Patel, and R. Muthyala, US Patent 5,260,180 (1993).
12. T. E. Kekhva, V. N. Lebedev, and I. V. Sokolova, *Zhur. Fiz. Khim.* **65**, 2036 (1991).
13. V. N. Bolshakov and M. A. Goryaev, *Opt. Tekh. Kino* **11**, 68 (1991); M. A. Goryaev, T. B. Kolesova, M. I. Timokhina, and I. M. Gulkova, in *Proceedings: Technology and Properties of Information Recording Materials*, Moscow, 1992, pp. 67ff.; M. A. Goryaev, in *Proceedings of the 1994 ICPS: Physics and Chemistry of Imaging Systems*, vol. 1, IS&T, Springfield, VA, 1994, p. 360.
14. (a) V. Vand, A. Atkins, and R. K. Campbell, *Acta Cryst.* **2**, 398 (1949); (b) M. Ikeda and Y. Iwata, *Photogr. Sci. Eng.* **24**, 273 (1980).
15. T. C. W. Mak, W.-H. Yip, C. H. L. Kennard, G. Smith, and E. J. O'Reilly, *Aust. J. Chem.* **139**, 541 (1986); X.-M. Chen and T. C. W. Mak, *J. Chem. Soc., Dalton Trans.* 1219 (1991).
16. (a) D. R. Whitcomb, W. C. Frank, R. D. Rogers, B. P. Tolochko, S. V. Chernov, and S. G. Nikitenko, *Proceedings: IS&T's 49th Annual Conference*, IS&T, Springfield, VA, 1996, pp. 426ff.; (b) B. P. Tolochko, S. V. Chernov, S. G. Nikitenko, and D. R. Whitcomb, *Nucl. Inst. and Meth. Phys. Res., A*, accepted for publication.
17. L. P. Burleva, Ph.D. Thesis, Siberian Branch of the Russian Academy of Sciences, Novosibirsk, 1989, p. 18.
18. A. E. Gvozdev, *Ukrain. Fiz. Zhurn.* **24**, 1856 (1979).
19. R. Hoffmann, *Solids and Surfaces*, VCH Publishers, New York, 1988.
20. A. von Koenig, H. Kampfer, E. M. Brinckmann, and F. C. Heugebaert, US Patent 3,933,507 (1976); I. H. Leubner, *Res. Discl.* **152**, 61 (Dec. 1976).
21. (a) R. Tausch-Tremel, A. Henglein, and J. Lillie, *Ber. Bunsenges. Phys. Chem.* **82**, 1335 (1978); (b) M. Mostafavi, J.-L. Marignier, J. Amblard, and J. Belloni, *Radiat. Phys. Chem.* **34**, 605 (1989); (c) P. Mulvaney and A. Henglein, *J. Phys. Chem.* **94**, 4182 (1990); (d) M. Mostafavi, M. O. Delcourt, N. Kéghouche, and G. Picq, *Radiat. Phys. Chem.* **40**, 445 (1992); (e) M. Kobayashi and H. Sato, *Chem. Lett.* 1659 (1993); (f) E. Janata, A. Henglein, and B. G. Ershov, *J. Phys. Chem.* **98**, 10888 (1994).
22. A. J. Nozik and R. Memming, *J. Phys. Chem.* **100**, 13061 (1996).
23. M. W. Peterson, J. A. Turner, C. A. Parsons, A. J. Nozik, D. J. Arent, C. Van Hoof, G. Borghs, R. Houdre, and H. Morkoc, *Appl. Phys. Lett.* **53**, 2666 (1988); B. Deveaud, J. Shah, T. C. Damen, B. Lambert, and A. Regreny, *Phys. Rev. Lett.* **58**, 2582 (1987).
24. M. Chadha, M. E. Dunnigan, M. R. V. Sahyun, and T. Ishida, *J. Appl. Phys.*, submitted for publication.
25. W. N. Delgass, G. L. Haller, R. Kellerman, and J. H. Lumsford, *Spectroscopy in Heterogeneous Catalysis*, Academic Press, New York, 1979, pp. 128ff.
26. M. R. V. Sahyun, S. E. Hill, N. Serpone, R. Danesh, and D. K. Sharma, *J. Appl. Phys.* **79**, 8030 (1996).
27. (a) M. R. V. Sahyun and S. E. Hill, unpublished results; (b) S. H. Ehrlich, *J. Imaging Sci.* **37**, 73 (1993).
28. (a) M. Simons, US Patent 3,839,049 (1972); (b) J. M. Winslow and I. R. Maw, US Patent 4,161,408 (1979); (c) H. W. Altland and D. D. F. Shiao, US Patent 4,351,896 (1982); (d) K. A. Penfound, US Patent 4,476,220 (1984).
29. Yu. E. Usanov and T. N. Kolesova, *J. Imaging Sci. Tech.* **40**, 104 (1996).
30. A. P. Marchetti and R. S. Eachus, *Adv. Photochem.* **17**, 145 (1991) and references cited therein.
31. R. M. Gibb, G. J. Rees, B. W. Thomas, B. L. H. Wilson, B. Hamilton, D. R. Wright, and N. F. Mott, *Phil. Mag.* **36**, 1021 (1977).
32. U. Kreibitz, *J. Phys.* **F4**, 999 (1974); R. Tausch-Tremel, A. Henglein, and J. Lillie, *Ber. Bunsenges. Phys. Chem.* **82**, 1335 (1978); T. Welker, *ibid.* **82**, 40 (1978).
33. N. Serpone, D. Lawless, B. Lenet, and M. R. V. Sahyun, *J. Imaging Sci. Tech.* **37**, 517 (1993); N. Serpone, D. Lawless and M. R. V. Sahyun, *Supramol. Chem.* **5**, 15 (1995).
34. (a) R. J. Araujo and N. F. Borelli, in *Optical Properties of Glass*, D. R. Uhlmann and N. J. Kreidl, Eds., American Ceramic Society, Westerville, OH, 1991, pp. 125ff.; (b) T. P. Seward, III, *J. Noncryst. Solids*, **40**, 499 (1980); *J. Appl. Phys.* **46**, 689 (1975).
35. N. F. Borelli, J. B. Chodak, and G. B. Hares, *J. Appl. Phys.* **50**, 5978 (1979).
36. (a) P. J. Hillson and E. A. Sutherns, in *Theory of the Photographic Process*, 3rd ed., T. H. James, Ed., Macmillan, New York, 1967, pp. 155ff. and references cited therein; (b) R. W. Gurney and N. F. Mott, *Proc. Roy. Soc. (London), Ser. A* **164**, 151 (1938).
37. T. Petrova and N. Pangelova, *J. Imaging Sci.* **33**, 173 (1989).
38. L. P. Burleva, V. M. Andreev and V. V. Boldyrev, *J. Thermal Anal.* **33**, 735 (1988) and references cited therein.
39. S. E. Hill, M. B. Mizen, M. R. V. Sahyun, and Yu. E. Usanov, *J. Imaging Sci. Tech.* **40**, 568 (1996).
40. A. Sidelnikov, Institute for Solid State Chemistry, Novosibirsk, Russia, private communication; see also ref. 39.
41. M. B. Mizen, in ref. 8a, p. 34.
42. T. H. James, in ref. 36a, pp. 333, and references cited therein.
43. Yu. E. Usanov, T. B. Kolesova, L. P. Burleva, M. R. V. Sahyun, and D. R. Whitcomb, in ref. 8, p. 42.
44. E. V. Boldyreva, *Reactivity of Solids* **8**, 269 (1990); V. V. Boldyrev, *ibid.* **40**, 1041 (1993).
45. S. M. Shor, in ref. 5a, pp. 442ff.
46. (a) B. H. Carroll, *Preprints of Paper Summaries: 27th Annual Conference, SPSE, SPSE*, Washington, DC, 1974; (b) T. L. Beaupré, R. R. Jasper, D. A. Turbide, and M. T. Williams, *Photogr. Sci. Eng.* **18**, 535 (1974). See also ref. 51.
47. U. Nickel, N. Rühl and B. M. Zhou, *Z. Phys. Chem.* **NF148**, 33 (1986).
48. X. Zhai and S. Efrima, *J. Phys. Chem.* **100**, 1779 (1996).
49. Z.-Y. Huang, G. Mills and B. Hajek, *J. Phys. Chem.* **97**, 11542 (1993).
50. T. H. James, in ref. 36a, p. 352.
51. M. R. V. Sahyun, *Photogr. Sci. Eng.* **19**, 38 (1975).
52. W. Jaenicke, *Photogr. Sci. Eng.* **6**, 185 (1962); H. J. Metz, *J. Photogr. Sci.* **20**, 111 (1972); see also M. R. V. Sahyun, *J. Chem. Educ.* **51**, 72 (1974).
53. (a) N. F. Mott, *Phot. J.* **88B**, 119 (1949); (b) C. R. Berry, *Photogr. Sci. Eng.* **13**, 65 (1977).
54. B. Bokhonov, Institute for Solid State Chemistry, Novosibirsk, Russia, private communication; see also ref. 9.